Physics Letters B 750 (2015) 45–52

Contents lists available at ScienceDirect

Physics Letters B

www.elsevier.com/locate/physletb

Analytic Bjorken flow in one-dimensional relativistic magnetohydrodynamics

Victor Roy [a,*], Shi Pu [a], Luciano Rezzolla [a,b], Dirk Rischke [a]

[a] Institute for Theoretical Physics, Goethe University, Max-von-Laue-Str. 1, 60438 Frankfurt am Main, Germany
[b] Frankfurt Institute for Advanced Studies, Ruth-Moufang-Str. 1, 60438 Frankfurt am Main, Germany

ARTICLE INFO

Article history:
Received 25 June 2015
Received in revised form 5 August 2015
Accepted 19 August 2015
Available online 24 August 2015
Editor: J.-P. Blaizot

ABSTRACT

In the initial stage of relativistic heavy-ion collisions, strong magnetic fields appear due to the large velocity of the colliding charges. The evolution of these fields appears as a novel and intriguing feature in the fluid-dynamical description of heavy-ion collisions. In this work, we study analytically the one-dimensional, longitudinally boost-invariant motion of an ideal fluid in the presence of a transverse magnetic field. Interestingly, we find that, in the limit of ideal magnetohydrodynamics, i.e., for infinite conductivity, and irrespective of the strength of the initial magnetization, the decay of the fluid energy density e with proper time τ is the same as for the time-honoured "Bjorken flow" without magnetic field. Furthermore, when the magnetic field is assumed to decay $\sim \tau^{-a}$, where a is an arbitrary number, two classes of analytic solutions can be found depending on whether a is larger or smaller than one. In summary, the analytic solutions presented here highlight that the Bjorken flow is far more general than formerly thought. These solutions can serve both to gain insight on the dynamics of heavy-ion collisions in the presence of strong magnetic fields and as testbeds for numerical codes.

1. Introduction

Very intense magnetic fields of the order of $B \sim 10^{18}$–10^{19} G are produced orthogonal to the direction of motion in a typical non-central Au–Au collision at top RHIC energy (i.e., with a centre-of-momentum energy per nucleon pair of $\sqrt{s_{\rm NN}} \simeq 200\,{\rm GeV}$). Recent studies show that the strength of the produced magnetic field grows approximately linearly with the centre-of-momentum energy of the colliding nucleons [1–3]. It is now an experimentally well-established fact that in high-energy nucleus–nucleus collisions a very hot and dense phase of nuclear matter composed of quarks and gluons is formed. This hot and dense form of nuclear matter is also known as quark–gluon plasma (QGP). In the presence of a strong magnetic field as created in heavy-ion collisions, a charge current will be induced in the QGP, leading to what is known as the "chiral magnetic effect" (CME) [3]. At the same time, particles with the same charge but different chirality will also be separated, yielding what is called the "chiral separation effect" (CSE). A density wave induced by these two effects, called the "chiral magnetic wave" [4], is suggested to break the degeneracy between the elliptic flows of positive and negative pions [5]. Moreover, it has also been found that there exists a deep connection between these effects and the Berry phase in condensed matter [6–8]. Research on these topics is developing rapidly and a series of recent reviews and references can be found in Refs. [9–11].

The initial electric fields are also found to be quite large in event-by-event simulations of heavy-ion collisions [2]. Such electric fields induce other novel effects such as the "chiral electric separation effect" (CESE) and the "chiral electric wave" (CEW), which represent chiral currents and density waves induced by the electric fields, respectively [12,13]. When the electric field is perpendicular to the magnetic field, just like for the Hall effect, a chiral current is expected, called the "chiral Hall separation effect" (CHSE), which might cause an asymmetric charge distribution in rapidity [14].

Relativistic hydrodynamics has been proven to be quite successful in describing the experimentally measured azimuthal distribution of particle emission in non-central nucleus–nucleus collisions [15–20]. It is then important to understand the effect of initial large magnetic fields on the fluid evolution. To this scope one needs a numerical code that solves the equations of $(3+1)$-dimensional relativistic magnetohydrodynamics (MHD). There is consensus that due to very high velocities of the charges inside the colliding nuclei (i.e., with Lorentz factors $\gamma \sim 100$ for

* Corresponding author.
E-mail address: roy@th.physik.uni-frankfurt.de (V. Roy).

http://dx.doi.org/10.1016/j.physletb.2015.08.046

collisions at $\sqrt{s_{\rm NN}} = 200\,{\rm GeV}$), the magnetic fields decay very rapidly (i.e., decreasing by $\sim$ 3 orders of magnitude within a timescale $\sim 1\,{\rm fm}$ for $\sqrt{s_{\rm NN}} = 200\,{\rm GeV}$ Au–Au collisions) before the system reaches local thermal equilibrium and the fluid description is applicable. However, the presence of a medium with finite electrical conductivity can substantially delay the decay of the magnetic field [21–23].

Lattice-QCD simulations and theoretical models show that the QGP possesses a finite temperature-dependent electrical conductivity [24,25]. However, the interaction of the initial magnetic field with the QGP and its subsequent evolution is still an open issue and a topic of current research. An estimate of the relative importance of an external magnetic field on the fluid evolution can be obtained from the dimensionless quantity $\sigma \equiv B^2/e$, which represents the ratio of the magnetic-field energy density to the fluid energy density e. Clearly, values of $\sigma \gtrsim 1$ indicate that one must consider the effect of the magnetic field on the fluid evolution. For a typical mid-central (i.e., with impact parameter $b \sim 10\,{\rm fm}$) Au–Au collision at top RHIC energy ($\sqrt{s_{\rm NN}} = 200\,{\rm GeV}$) the average magnetic field can be as high as $\sim 10\, m_\pi^2 \sim 10^{19}$ G [1,2], where m_π is the pion mass, which corresponds to an energy density of $\sim 5\,{\rm GeV/fm^3}$. Hydrodynamical model studies show that the initial energy density for such cases is $\sim 10\,{\rm GeV/fm^3}$, thus implying $\sigma \sim 1$ under these conditions.

We note that the estimates made above are based on the assumption that the magnetic field (evaluated at time $\tau = 0\,{\rm fm}$) remains unchanged until the fluid starts expanding after reaching local thermal equilibrium at $\tau_0 \sim 0.5\,{\rm fm}$. We also note that the estimate of σ as given above is based on the event-averaged values for the initial magnetic field and energy density of the fluid. However, the situation can be very different. In fact, it is possible that the initial energy density distribution is very "lumpy". Under these conditions, the produced magnetic fields also show large variations and can be very large in some places where the corresponding fluid energy–density is small. In these cases, even for a quickly decaying initial magnetic field we may locally have $\sigma > 1$ up to the time when the hydrodynamical expansion starts.

It is not the goal of this work to investigate the temporal evolution of the magnetic field produced in heavy-ion collisions. Rather, we concentrate here on the special case of one-dimensional, longitudinally boost-invariant fluid expansion à la Bjorken [26] under the influence of an external magnetic field which is transverse to the fluid velocity. In our analysis the evolution of the magnetic field is either regulated from the flux-freezing condition in ideal MHD or imposed in terms of a parameterized power law in proper time. The ultimate goal is that of finding analytic solutions for this flow that can be used both to gain insight in the dynamics of ultrarelativistic MHD flows as well as an effective test for more complex and realistic numerical codes (see also Ref. [28] for a work with similar intentions).

The paper is organized as follows. Section 2 introduces our mathematical setup, while Section 3 presents the energy–density evolution when considering two representative prescriptions for the evolution of the magnetic field. A discussion of our main results is presented in Section 4, while a conclusive summary is given in Section 5.

Following the predominant convention in relativistic hydrodynamics of heavy-ion collisions, we use a timelike signature $(+,-,-,-)$ and a system of units in which $\hbar = c = k_{\rm B} = 1$. Greek indices are taken to run from 0 to 3, Latin indices from 1 to 3 and we adopt the standard convention for the summation over repeated indices. Finally, we indicate three-vectors as bold face letter with an arrow and use bold letters without an arrow to denote four-vectors and tensors.

2. Mathematical setup

We consider an ideal but magnetized relativistic fluid with an energy–momentum tensor given by[1] [29–32]

$$T^{\mu\nu} = \left(e + p + B^2\right) u^\mu u^\nu - \left(p + \frac{B^2}{2}\right) g^{\mu\nu} - B^\mu B^\nu\,, \tag{1}$$

where e, p, and $\boldsymbol{u}$ are the fluid energy density, pressure, and four-velocity, respectively. Since our considerations are restricted to special-relativistic flows, the metric tensor is that of flat spacetime, i.e., $g^{\mu\nu} = \eta^{\mu\nu} = {\rm diag}(1,-1,-1,-1)$. Here $B^\mu = \frac{1}{2}\epsilon^{\mu\nu\alpha\beta}F_{\nu\alpha}u_\beta$ is the magnetic field in the frame moving with the velocity u_β, $\epsilon^{\mu\nu\alpha\beta}$ is the completely antisymmetric four tensor, $\epsilon^{0123} = \sqrt{\det|g|}$. The magnetic field four-vector B^μ is a spacelike vector with modulus $B^\mu B_\mu = -B^2$, and orthogonal to u^μ, i.e., $B^\mu u_\mu = 0$, where $B = |\vec{\boldsymbol{B}}|$ and $\vec{\boldsymbol{B}}$ is the magnetic field three-vector in the frame moving with four-velocity u^μ.

As mentioned above, we are here interested in obtaining analytic solutions representing the MHD extension of one-dimensional Bjorken flow along the z-direction with velocity $u^\mu = \gamma\,(1,0,0,v_z)$, where $v_z \equiv z/t$ [26]. Hence, hereafter we will assume the special case of a fluid flow in which the external magnetic field $\vec{\boldsymbol{B}}$ is directed along the direction transverse to the fluid velocity $\vec{\boldsymbol{v}}$; as remarked above, this represents a rather good approximation of what happens in a typical non-central Au–Au collision at top RHIC energy. This setup is also known as "transverse MHD", since the magnetic field is contained in the transverse (x,y) plane [27]. In addition, since the fluid is expected to be ultrarelativistic, the rest-mass contributions to the equation of state (EOS) can be neglected and the pressure is simply proportional to the energy density, i.e.,

$$p = c_s^2\, e = \frac{1}{3}\, e\,, \tag{2}$$

where c_s is the local sound speed which is assumed to be constant. The second equality in Eq. (2) refers to the case of an ultrarelativistic gas, or isotropic "radiation fluid" [33], where $c_s = 1/\sqrt{3}$ and which we will often consider in the remainder of this work.

Rather than using a standard Cartesian coordinate system (t,x,y,z), for longitudinally boost-invariant flow it is more convenient to adopt Milne coordinates,

$$(\tau\,, x, y, \eta) \equiv \left(\sqrt{t^2 - z^2}, x, y, \frac{1}{2}\ln\left(\frac{t+z}{t-z}\right)\right). \tag{3}$$

In these coordinates, the convective derivative is defined as $u^\mu\partial_\mu = \partial_\tau$, while the expansion scalar takes the simple form $\Theta \equiv \partial_\mu u^\mu = \tau^{-1}$.

As customary, the projection of the energy–momentum conservation equation $\partial_\nu T^{\mu\nu} = 0$ along the fluid four-velocity,

$$u_\mu \partial_\nu T^{\mu\nu} = 0\,, \tag{4}$$

will express the conservation of energy. After some steps that can be found in Appendix A, we obtain the following energy–conservation equation

$$\partial_\tau\left(e + \frac{B^2}{2}\right) + \frac{e + p + B^2}{\tau} = 0\,. \tag{5}$$

Similarly, the projection of the energy–momentum conservation equation onto the direction orthogonal to $\boldsymbol{u}$,

$$(\eta_{\mu\nu} - u_\mu u_\nu)\partial_\alpha T^{\alpha\nu} = 0 \tag{6}$$

[1] Note that expression (1) for the energy–momentum tensor is different from the one usually adopted in general-relativistic MHD (GRMHD) formulations and that we briefly review in Appendix A.

leads to the momentum–conservation, or Euler, equation (see Appendix A),

$$\left(e+p+B^2\right)\partial_\tau u_\mu - (\eta_{\mu\nu}-u_\mu u_\nu)\partial^\nu\left(p+\frac{B^2}{2}\right)=0\,. \tag{7}$$

Note that for $\mu=\eta$, it reads

$$\frac{\partial}{\partial\eta}\left(p+\frac{1}{2}B^2\right)=0\,, \tag{8}$$

thus showing that all thermodynamical variables depend only on τ and are otherwise uniform in space. Considering instead $\mu=x,y$, Eq. (7) gives the MHD equivalent of the Euler equation

$$\partial_\tau u_i - \frac{1}{e+p+B^2}\partial_i\left(p+\frac{1}{2}B^2\right)=0\,. \tag{9}$$

With a uniform pressure and a magnetic field that depends only on τ, the second term in Eq. (9) will vanish, thus implying that if the velocities in the x- and y-directions are initially zero, they will remain so also at later times (i.e., $\partial_\tau u_i=0$).

3. Energy–density evolution

This section is dedicated to the discussion of two different cases for the evolution of the energy density depending on whether the magnetic field evolves according to the ideal-MHD limit (Section 3.1) or whether it follows an arbitrary power–law decay in proper time (Section 3.2).

3.1. Ideal-MHD limit

The solution of Eq. (5) requires the knowledge of the evolution of the magnetic field and hence of the induction equation. In the limit of infinite electrical conductivity, i.e., in the ideal-MHD limit, the magnetic field obeys the frozen-flux (or Alfvén) theorem and is thus simply advected with the fluid. In this case, setting $B\equiv\sqrt{B^iB_i}$, the induction equation takes the simple form

$$B(\tau)=B_0\frac{\rho}{\rho_0}\,, \tag{10}$$

where τ_0 is taken to mark the beginning of the fluid expansion and $\rho_0\equiv\rho(\tau_0)$, $B_0\equiv B(\tau_0)$, are the initial fluid rest-mass density and magnetic field, respectively.

As written, Eq. (10) is of little use. In relativistic heavy-ion collisions, in fact, the net-baryon number is vanishingly small at mid-rapidity and the flux-freezing condition expressed by Eq. (10) needs to be modified to account for this. As we show in Appendix B, this is rather easy to do and yields, for an ultrarelativistic fluid with EOS (2), an evolution equation for the magnetic field,

$$\vec{\boldsymbol{B}}(\tau)=\vec{\boldsymbol{B}}_0\frac{s}{s_0}=\vec{\boldsymbol{B}}_0\left(\frac{e}{e_0}\right)^{1/(1+c_s^2)}=\vec{\boldsymbol{B}}_0\left(\frac{e}{e_0}\right)^{3/4}\,, \tag{11}$$

where s is the entropy density, $s_0\equiv s(\tau_0)$, and the third equality in Eq. (11) refers to the case $c_s=1/\sqrt{3}$. Note that the second equality in Eq. (11) is the result of the first law of thermodynamics and reflects the relation between entropy and energy densities in an ultrarelativistic fluid [33].

Using Eq. (11) in Eq. (5), we obtain

$$\partial_\tau\left[e+\frac{B_0^2}{2}\left(\frac{e}{e_0}\right)^{2/(1+c_s^2)}\right]+\frac{e+p+B_0^2\,(e/e_0)^{2/(1+c_s^2)}}{\tau}=0\,, \tag{12}$$

which can also be written in dimensionless form as

$$\partial_\tau\left[\tilde{e}+\frac{\sigma_0}{2}\tilde{e}^{2/(1+c_s^2)}\right]+\frac{\tilde{e}+\tilde{p}+\sigma_0\tilde{e}^{2/(1+c_s^2)}}{\tau}=0\,, \tag{13}$$

where $\tilde{e}\equiv e/e_0$, $\tilde{p}\equiv p/e_0$, and $\sigma_0\equiv B_0^2/e_0$.

Not surprisingly, in the limit of vanishing magnetic field, i.e., for $\sigma_0\to 0$, Eq. (13) takes the form of the Bjorken expansion, for which the energy density evolves according to

$$\partial_\tau\tilde{e}=-\frac{\tilde{e}+\tilde{p}}{\tau}=-(1+c_s^2)\frac{\tilde{e}}{\tau}\,, \tag{14}$$

where the second equality is written using the EOS (2).

Using again Eq. (2), we find that both terms on the left-hand side of Eq. (13) contain a common factor that can be removed: $1+\sigma_0\tilde{e}^{(1-c_s^2)/(1+c_s^2)}/(1+c_s^2)$. As a result, Eq. (13) can be written as

$$\partial_\tau\,\tilde{e}=-(1+c_s^2)\frac{\tilde{e}}{\tau}=-\frac{4}{3}\frac{\tilde{e}}{\tau}\,, \tag{15}$$

where the second equality refers to the more specific case of an EOS with $c_s=1/\sqrt{3}$.

Thus, Eq. (15), which was derived within ideal MHD, coincides with Eq. (14), which instead refers to Bjorken flow in the absence of an external magnetic field. After a more careful look, this result is not so surprising. In the ideal-MHD limit, in fact, the ratios $\vec{\boldsymbol{B}}/s$ and thus $\vec{\boldsymbol{B}}/e^{1/(1+c_s^2)}$ are conserved [cf. Eq. (11)] and although the total energy density will be larger in the presence of a magnetic field, the evolution of the fluid energy density will not be affected by the magnetic field which will be equally diluted as the fluid expansion takes place. This is essentially because the magnetic field has no active role in ideal MHD, but is simply passively advected in the expansion. Stated differently, a Bjorken flow is more general than formerly thought, as it applies not only to purely hydrodynamical flows, but also to transverse MHD flows. To the best of our knowledge, this result, albeit natural, was not remarked before in the literature.

Equation (15) has an analytic solution of the form

$$\tilde{e}(\tau)=c\tau^{-1/(1+c_s^2)}=\left(\frac{\tau_0}{\tau}\right)^{1+c_s^2}=\left(\frac{\tau_0}{\tau}\right)^{4/3}\,, \tag{16}$$

where c is a constant that could be chosen, for instance, from the initial value of the energy density: $\tilde{e}_0\equiv\tilde{e}(\tau_0)=1$, and where the last equality again refers to $c_s=1/\sqrt{3}$. In the light of the remarks made above, it follows that Eq. (16) is also the solution for the energy density for Bjorken flow without magnetic field, cf. Eq. (14).

Two final remarks: first, we note that combining Eqs. (11) and (16), it is easy to see that the evolution of the magnetic field in this case will be

$$\tilde{B}(\tau)\equiv\frac{B(\tau)}{B_0}=\tilde{e}^{1/(1+c_s^2)}=\tilde{e}^{3/4}=\frac{\tau_0}{\tau}\,. \tag{17}$$

Second, our conclusion that the Bjorken flow is recovered in transverse MHD could have been reached also using entropy conservation and the Maxwell equations as long as the thermodynamical relations are not affected by the presence of a magnetic field (zero magnetization vector), i.e., as long as $de=Tds$, where T is the temperature [34]. In this case the derivation does not even require the specification of an EOS.

3.2. Power-law decay

Next, we explore cases where the external magnetic field does not vary according to the ideal-MHD flux-freezing condition (11), but has a different temporal evolution. Because we are in search

of analytic solutions, we consider here a rather simple prescription and, in particular, one in which the magnetic field follows a power–law decay in proper time, i.e.,

$$\vec{B}(\tau) = \vec{B}_0 \left(\frac{\tau_0}{\tau}\right)^a , \tag{18}$$

where a is a constant. Clearly, expression (18) is a simple ansatz but, as remarked in Eq. (17), it is sufficiently realistic to include the ideal-MHD case when $a = 1$. In addition, the range $a > 1$, i.e., of magnetic-field decay steeper than the ideal-MHD case, can be taken as a phenomenological description of a resistive regime. Under these conditions, in fact, a finite electrical conductivity will lead to a more rapid decay of the magnetic field and, in turn, to a slower decay of the fluid energy density, which is "heated up" by the decaying field [cf. Eq. (20)].

Let us start by considering the equation of energy conservation (5), which for a general EOS of the form (2) and a magnetic-field evolution given by Eq. (18) yields

$$\partial_\tau \left[\tilde{e} + \frac{\sigma_0}{2} \left(\frac{\tau_0}{\tau}\right)^{2a} \right] + \left(1 + c_s^2\right) \frac{\tilde{e}}{\tau} + \frac{\sigma_0}{\tau} \left(\frac{\tau_0}{\tau}\right)^{2a} = 0 . \tag{19}$$

It is not difficult to find the analytic solution of this equation with initial condition $\tilde{e}_0 = 1$,

$$\tilde{e}(\tau) = \left(\frac{\tau_0}{\tau}\right)^{1+c_s^2} + \sigma_0 \frac{1-a}{1+c_s^2-2a} \left[\left(\frac{\tau_0}{\tau}\right)^{1+c_s^2} - \left(\frac{\tau_0}{\tau}\right)^{2a} \right] . \tag{20}$$

Once again, it is possible to see that in the limit of vanishing magnetization $\sigma_0 \to 0$, Eq. (20) coincides with the solution (16) for Bjorken flow. Furthermore, for $\sigma_0 \neq 0$ but $a = 1$, the solution (20) also coincides with Eq. (16), thus highlighting that Eq. (18) with $a = 1$ represents the evolution equation for a magnetic field in the ideal-MHD limit.

Note that, for the second term in Eq. (20), the sign of the expression in brackets divided by $1 + c_s^2 - 2a$ is always negative (remember that $c_s^2 \leq 1$ by causality). Thus, for the case $a > 1$ the second term is always positive. As a result, it always leads to a slower decay (and sometimes, as we will show below, even to an intermittent increase) of the fluid energy density than in the case $a = 1$. Viceversa, for $a < 1$ the second term in Eq. (20) is always negative, leading to a faster decay than in the case $a = 1$.

Equation (20) seems to have a divergent behaviour at $a = (1 + c_s^2)/2$, but this is only a first impression. We demonstrate in Appendix C that in the limit $a \to (1 + c_s^2)/2$,

$$\lim_{a \to (1+c_s^2)/2} \frac{(\tau_0/\tau)^{1+c_s^2} - (\tau_0/\tau)^{2a}}{1 + c_s^2 - 2a} = \left(\frac{\tau_0}{\tau}\right)^{1+c_s^2} \ln\left(\frac{\tau_0}{\tau}\right) . \tag{21}$$

Collecting things, the final solution of the energy–conservation equation (19) for $a = (1 + c_s^2)/2$ is

$$\tilde{e}(\tau) = \left(\frac{\tau_0}{\tau}\right)^{1+c_s^2} + \sigma_0 \frac{1-c_s^2}{2} \left(\frac{\tau_0}{\tau}\right)^{1+c_s^2} \ln\left(\frac{\tau_0}{\tau}\right) . \tag{22}$$

Note that for $\tau \geq \tau_0$ the second term on the right-hand side of Eq. (22) is negative, hence increasing the decay of the fluid energy density with respect to the $a = 1$ case. Furthermore, while in the ideal-MHD case the solution $\tilde{e} = 0$ is obtained only asymptotically, for $a = (1 + c_s^2)/2$ this extreme case is obtained after a finite time $\bar{\tau} = \tau_0 e^{2/[(1-c_s^2)\sigma_0]}$.

In summary, Eqs. (20) and (22) represent the solutions to Eq. (19); furthermore, since Eq. (20) comprises also the case $a = 1$, these equations provide a rather complete description of the full solution to the energy–conservation equation (19). As an example, we quote the solutions for $c_s^2 = 1/3$. For $a \neq 2/3$,

$$\tilde{e}(\tau) = \left(\frac{\tau_0}{\tau}\right)^{4/3} + \frac{\sigma_0}{2} \frac{1-a}{2/3-a} \left[\left(\frac{\tau_0}{\tau}\right)^{4/3} - \left(\frac{\tau_0}{\tau}\right)^{2a} \right] , \tag{23}$$

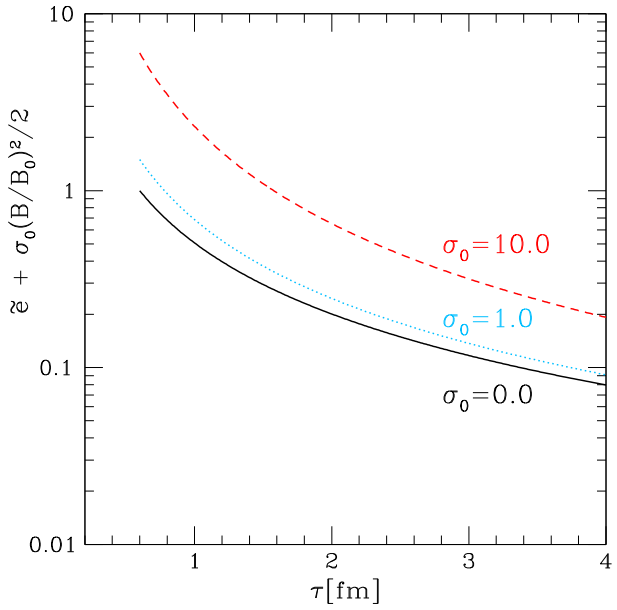

Fig. 1. Evolution of the normalized total energy density $\tilde{e} + \frac{1}{2}\sigma_0(B/B_0)^2$. Different lines refer to different values of the initial magnetization, ranging from $\sigma_0 = 0$ (solid black line) up to cases with initial magnetization of $\sigma_0 = 1$ (light-blue dotted line) and $\sigma_0 = 10$ (red dashed line). Note that the fluid energy density decays like $\tau^{-4/3}$ for all values of σ_0, i.e., as in traditional Bjorken flow. (For interpretation of the references to colour in this figure legend, the reader is referred to the web version of this article.)

and for $a = 2/3$,

$$\tilde{e}(\tau) = \left(\frac{\tau_0}{\tau}\right)^{4/3} + \frac{\sigma_0}{3} \left(\frac{\tau_0}{\tau}\right)^{4/3} \ln\left(\frac{\tau_0}{\tau}\right) . \tag{24}$$

4. Discussion

This section is devoted to a discussion of the various analytic solutions found in the previous section. For the sake of definiteness, we will always use the value $c_s^2 = 1/3$. We start by considering the ideal-MHD case, in which case the time evolution of the energy density and the magnetic field is given by Eqs. (16) and (17), respectively. These solutions are shown in Fig. 1 which reports the evolution of the normalized total energy density $\tilde{e} + \frac{1}{2}\sigma_0(B/B_0)^2$ for $\tau_0 = 0.6\,\text{fm}$. Different lines refer to different values of the initial magnetization, ranging from $\sigma_0 = 0$ (Bjorken flow without magnetic field; black solid line) up to cases with initial magnetization of $\sigma_0 = 1$ (light-blue dotted line) and $\sigma_0 = 10$ (red dashed line). As already discussed in the previous section, the evolution of the fluid energy density does not depend on σ_0 [cf. Eq. (16)] and scales like $\tau^{-4/3}$, while the magnetic energy density scales like τ^{-2}. As a result, increasing σ_0 (as we do in Fig. 1) only adds energy density to the system, but does not alter the temporal evolution of the fluid energy density.

Having considered the simple case $a = 1$, we next discuss the behaviour of the solutions when the magnetic field varies according to the more general power law (18). We have already mentioned that $a > 1$ corresponds to the case when the magnetic field decays faster than in the ideal-MHD limit and could therefore be associated to a resistive regime. Conversely, a magnetic-field evolution with $a < 1$ would correspond to a decay that is slower than in the ideal-MHD limit. As the case $a = 1$ is the limit of infinite conductivity, and thus of a maximal magnetic induction, it is at first sight hard to imagine how to produce a magnetic field that decays even slower than in the ideal-MHD case. However, in heavy-ion collisions the remnants of the colliding nucleons can give an additional contribution to the magnetic field, slowing down its de-

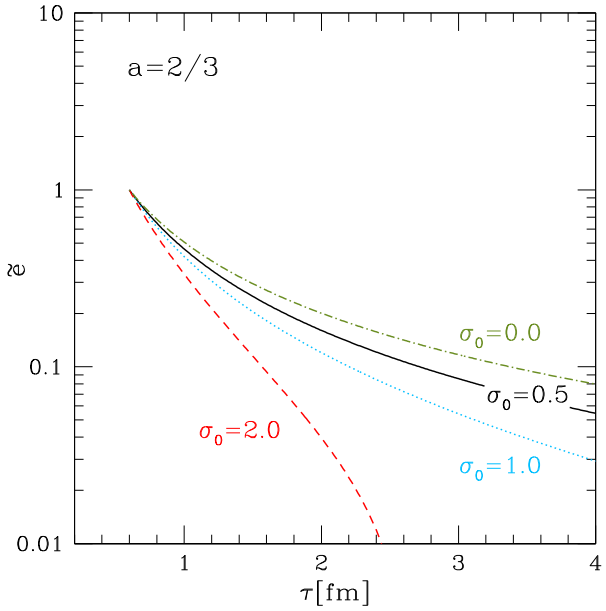

Fig. 2. Evolution of the normalized fluid energy density $\tilde{e}$ for $a = 2/3$. Different lines refer to different levels of the initial magnetization: $\sigma_0 = 0.5$ (black solid line), $\sigma_0 = 1$ (dotted light-blue line), and $\sigma_0 = 2.0$ (red dashed line). Note that the decrease of the energy density is always faster than in the ideal-MHD case (green dot-dashed curve). (For interpretation of the references to colour in this figure legend, the reader is referred to the web version of this article.)

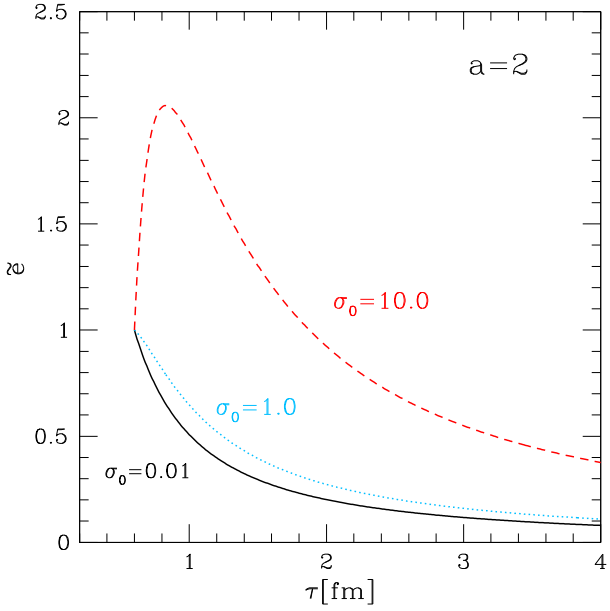

Fig. 3. Evolution of normalized fluid energy density $\tilde{e}$ for a magnetic field with a power–law decay $a = 2$. Also in this case, different lines refer to different levels of the initial magnetization, ranging from $\sigma_0 = 0.01$ (black solid line), $\sigma_0 = 1$ (light-blue dotted line), and $\sigma_0 = 10$ (red dashed line). Note the initial "heat-up" in the case of large magnetizations. (For interpretation of the references to colour in this figure legend, the reader is referred to the web version of this article.)

cay [2]. Thus, considering also the case $a < 1$ is reasonable in this context. Within this range, a particularly interesting solution is the one where $a = 2/3$, for in this case the general solution (23) needs to be replaced by the special solution (24).

Such a solution is shown in Fig. 2, which reports the evolution of $\tilde{e}$ for $a = 2/3$ and where different lines refer to different levels of the initial magnetization: $\sigma_0 = 0.5$ (black solid line), $\sigma_0 = 1$ (dotted light-blue line), and $\sigma_0 = 2.0$ (red dashed line). As already anticipated in the previous section, for $\tau > \tau_0$ the log term always reduces the value of $\tilde{e}$, leading to a faster decrease of the energy density when compared with the ideal-MHD limit (this is shown with a green dot-dashed line in Fig. 2). Furthermore, it is also clear that larger values of σ_0 will lead to a faster decrease in $\tilde{e}$, as shown in Fig. 2 (note that for $\sigma_0 = 2$, $\tilde{e} = 0$ at $\tau \simeq 2.7$ fm).

Finally, we consider in Fig. 3 the evolution of normalized fluid energy density $\tilde{e}$ in the case $a = 2$. Also in this case, different lines refer to different levels of the initial magnetization, $\sigma_0 = 0.01$ (black solid line), $\sigma_0 = 1$ (light-blue dotted line), and $\sigma_0 = 10$ (red dashed line). Because the second term in Eq. (23) is always positive, the evolution of the energy density is expected to be slower than in standard Bjorken flow (see also Fig. 4). At the same time, the second term in Eq. (23) is not a monotonically decreasing function of τ. As a result, it may produce even a temporary increase in the fluid energy density. This increase, which can be associated with a resistive "heating up" of the fluid, will depend on the values of σ_0 and a and will be larger for larger values of the latter. This is clearly shown in Fig. 3 for $\tau \lesssim 1$ fm in the case $\sigma_0 = 10.0$; after this time the evolution of the energy density is monotonically decreasing and asymptotically dominated by the term $\sim \tau^{-4/3}$.

As a way to summarize the various results presented so far we show in Fig. 4 the evolution of the normalized energy density $\tilde{e}$ in the different cases but keeping the initial magnetization fixed to $\sigma_0 = 1$. More specifically, we show the evolution for $a = 2/3$ (black solid line), $a = 1$ (light-blue dotted line), and $a = 2$ (red dashed line). Clearly, $\tilde{e}$ decreases more rapidly for $a = 2/3$ when compared to the case $a = 1$, whereas for $a = 2$ it initially decreases more slowly and then decays asymptotically at the same rate as for the ideal-MHD $a = 1$ case.

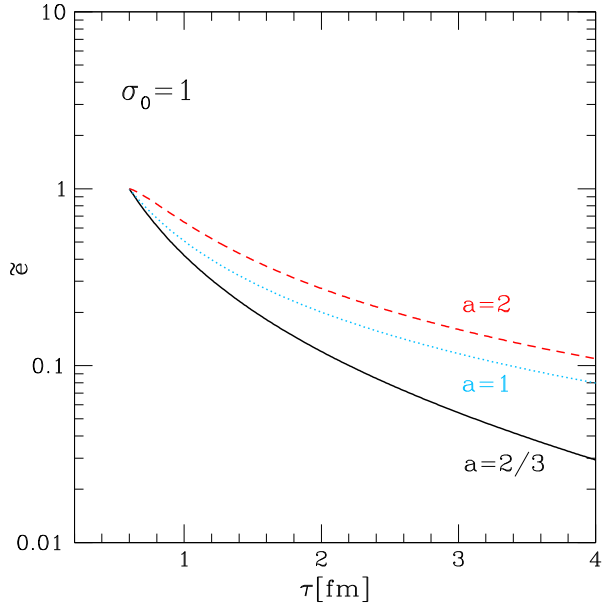

Fig. 4. Evolution of the normalized energy density $\tilde{e}$ in the different cases and when the initial magnetization is set to $\sigma_0 = 1$. Different lines refer to the evolution for $a = 2/3$ (black solid line), $a = 1$ (light-blue dotted line), and $a = 2$ (red dashed line). Clearly, $\tilde{e}$ decreases more rapidly for $a = 2/3$ when compared to the case $a = 1$, whereas for $a = 2$ it initially decays more slowly and then decays asymptotically at the same rate as for the ideal-MHD case $a = 1$. (For interpretation of the references to colour in this figure legend, the reader is referred to the web version of this article.)

5. Conclusions

Driven by the interest in exploring the effects of strong magnetic fields in the hydrodynamical description of relativistic heavy-

ion collisions, we have studied the evolution of the fluid energy density following the instant of the collision and considering an ultrarelativistic fluid with EOS $p = c_s^2 e$. Because we are mainly interested in finding analytic solutions, our setup is somewhat idealized and we have therefore considered one-dimensional, longitudinally boost-invariant flow with transverse magnetic field, i.e., a transverse-MHD flow. When no magnetic fields are present, this flow is known as the Bjorken flow [26] and although it represents a simplified prescription, it has served to gain significant insight on the dynamics of nucleus–nucleus collisions.

We have first considered the dynamics of a one-dimensional MHD flow in the limit of infinite electrical conductivity and found a somewhat surprising result, namely that in the ideal-MHD limit the Bjorken flow applies unmodified. The evolution of the fluid energy density, in fact, is regulated by the same equation found for Bjorken flow and thus with an analytic decay in proper time as $\tau^{-4/3}$. Of course large values of the initial magnetization will change the values of the total energy density, but the evolution of the fluid energy density will not be modified because of the passive role played by the magnetic field in this regime. This result widens considerably the range of applicability of the Bjorken model and shows that it can be used, unmodified, also to describe collisions in transverse MHD.

We have also considered the cases in which the magnetic-field evolution is not the one prescribed by the ideal-MHD limit but, rather, follows a power–law behaviour in proper time with exponent a. The solutions in this case need to be distinguished between the scenario in which the magnetic field decays more slowly than in the ideal-MHD case, i.e., for $a < 1$ and when the decay is more rapid, i.e., for $a > 1$. In the first scenario, which could be realized when remnants of the colliding nuclei slow down the decay of the magnetic field, the decay of the energy density is faster. Furthermore, the rate at which this decay takes place is determined entirely by the level of the initial magnetization and modelled in terms of the dimensionless magnetic-to-fluid energy $\sigma_0 \equiv B_0^2/e_0$. In the second scenario, which could be associated to a resistive regime in which magnetic field energy is converted to fluid energy via resistive losses, the evolution of the energy density is more complex. In the initial stages of the evolution, in fact, the fluid energy density may increase as it would in terms of a resistive "heating up" of the fluid. The amount of this increase depends on the magnetic field strength and dissipation and hence will increase with σ_0 and a. However, as the fluid further expands, its energy density will decrease with an asymptotic rate that is the same as in the Bjorken flow, i.e., $\propto \tau^{-4/3}$.

The work presented here could be extended in a number of ways. First, one could search for analytic solutions in one-dimensional MHD in a Landau-type flow scenario. Second, one can consider an explicitly finite electrical conductivity as the simplest model for a one-dimensional MHD flow with chiral fermions. Results on these topics will be presented in forthcoming papers.

Acknowledgements

V.R. and S.P. are supported by the Alexander von Humboldt Foundation, Germany. Partial support comes from "NewCompStar", COST Action MP1304 and the NSFC under grant No. 11205150.

Appendix A. Covariant derivative for Bjorken expansion

In this appendix we sketch briefly the steps that are needed to derive the energy– and momentum–conservation equations discussed in the main text. Before we start, we should comment about the notation used in defining the energy–momentum tensor (1). Bearing in mind that in general-relativistic calculations the standard choice for the signature is a spacelike one, i.e., $(-,+,+,+)$, the energy–momentum tensor in GRMHD is normally defined as [31,32]

$$T^{\mu\nu} = \left(e + p + b^2\right) u^\mu u^\nu + \left(p + \frac{b^2}{2}\right) g^{\mu\nu} - b^\mu b^\nu \,, \tag{A.1}$$

where $\boldsymbol{b}$ is the magnetic field four-vector measured in a comoving frame and has components given by

$$b^\mu = \left(\gamma\ \vec{\boldsymbol{v}} \cdot \vec{\boldsymbol{B}}, \frac{\vec{\boldsymbol{B}}}{\gamma} + \gamma\ \vec{\boldsymbol{v}} \cdot \vec{\boldsymbol{B}}\ \vec{\boldsymbol{v}}\right) , \tag{A.2}$$

with $\gamma \equiv 1/\sqrt{1-v^2}$ the Lorentz factor and $\vec{\boldsymbol{B}}$ is the magnetic field three-vector measured by an Eulerian (or normal) observer. The modulus of b^μ is then given by

$$b^2 \equiv b^\mu b_\mu = \frac{\vec{\boldsymbol{B}}^2}{\gamma^2} + \left(\vec{\boldsymbol{v}} \cdot \vec{\boldsymbol{B}}\right)^2 . \tag{A.3}$$

With this clarification in mind, we go back to our special-relativistic setting with energy–momentum (1) and consider the projection of the energy–momentum conservation equation $\partial_\nu T^{\mu\nu} = 0$ along the fluid four-velocity u^μ, which reads

$$\begin{aligned}
&u_\mu \partial_\nu T^{\mu\nu} = 0 \\
&u_\mu u^\mu u^\nu \partial_\nu \left(e + p + B^2\right) + \left(e + p + B^2\right) u_\mu \partial_\nu \left(u^\mu u^\nu\right) \\
&\quad - u_\mu \partial_\nu \left[\left(p + \frac{B^2}{2}\right) g^{\mu\nu}\right] - u_\mu \partial_\nu \left(B^\mu B^\nu\right) = 0 \,, \\
&u^\nu \partial_\nu \left(e + p + B^2\right) + \left(e + p + B^2\right) \partial_\nu u^\nu \\
&\quad - u^\nu \partial_\nu \left(p + \frac{B^2}{2}\right) + B^\mu B^\nu \partial_\nu u_\mu = 0 \,, \\
&\partial_\tau \left(e + p + B^2\right) + \frac{e + p + B^2}{\tau} - \partial_\tau \left(p + \frac{B^2}{2}\right) = 0 \,, \\
&\partial_\tau \left(e + \frac{B^2}{2}\right) + \frac{e + p + B^2}{\tau} = 0 \,,
\end{aligned} \tag{A.4}$$

where we have used Eq. (1), $u^\mu B_\mu = 0$ and $B^\nu \partial_\nu u_\mu = 0$, since $u_\mu = (u_0, 0, 0, u_z)$ and $B_\mu = \left(0, B_x, B_y, 0\right)$ in our transverse-MHD setup.

Similarly, the projection of the conservation equation $\partial_\nu T^{\mu\nu} = 0$ in the direction orthogonal to the fluid four-velocity gives

$$\begin{aligned}
&h_{\mu\nu} \partial_\alpha T^{\alpha\nu} = 0 \,, \\
&(e + p + B^2) h_{\mu\nu} \partial_\alpha (u^\alpha u^\nu) - h_{\mu\nu} \partial^\nu \left(p + \frac{B^2}{2}\right) \\
&\quad - h_{\mu\nu} \partial_\alpha (B^\alpha B^\nu) = 0 \,, \\
&(e + p + B^2) u^\alpha \partial_\alpha u_\mu - h_{\mu\nu} \partial^\nu \left(p + \frac{B^2}{2}\right) - B^\alpha \partial_\alpha B_\mu \\
&\quad - B_\mu \partial^\alpha B_\alpha + u_\mu u_\nu \partial_\alpha \left(B^\alpha B^\nu\right) = 0 \,, \\
&(e + p + B^2) \partial_\tau u_\mu - h_{\mu\nu} \partial^\nu \left(p + \frac{B^2}{2}\right) - B^\alpha \partial_\alpha B_\mu - B_\mu \partial^\alpha B_\alpha \\
&\quad - u_\mu B^\alpha B^\nu \partial_\alpha u_\nu = 0 \,,
\end{aligned} \tag{A.5}$$

where we have introduced $\boldsymbol{h}$ as the orthogonal projector to $\boldsymbol{u}$, i.e., $\boldsymbol{h} \cdot \boldsymbol{u} = 0$, where $h_{\mu\nu} \equiv \eta_{\mu\nu} - u_\mu u_\nu$. The last three terms vanish, because B_μ is assumed to be constant in transverse direction. This then leads to Eq. (7).

Appendix B. Frozen-flux theorem

In this appendix we show that the evolution of the magnetic field and of the entropy density are strictly related in the ideal-MHD limit. The arguments reported below are well known and can be found in a number of textbooks (e.g., Refs. [33,35]), but we recall them here for completeness. We start from the definition of the covariant (or Lagrangian or convective) time derivative given by

$$\frac{D}{Dt} \equiv \frac{\partial}{\partial t} + \vec{\boldsymbol{u}} \cdot \vec{\nabla}\,, \tag{B.1}$$

where $\vec{\boldsymbol{u}}$ is the fluid velocity. If $\vec{\boldsymbol{x}}$ is the position of a fluid element, this will be advected with the flow and hence have

$$\frac{D\vec{\boldsymbol{x}}}{Dt} = 0\,. \tag{B.2}$$

However, if $\vec{\boldsymbol{\xi}}$ is a vector separating two fluid elements at a given instant, the corresponding Lagrangian derivative will not be necessarily be zero, but is actually given by

$$\frac{D\vec{\boldsymbol{\xi}}}{Dt} = \vec{\boldsymbol{\xi}} \cdot \vec{\nabla}\vec{\boldsymbol{u}}\,. \tag{B.3}$$

Stated differently $D\vec{\boldsymbol{\xi}}/Dt = 0$ only for a fluid with uniform velocity $\vec{\boldsymbol{u}}$. In all other cases, the vector $\vec{\boldsymbol{\xi}}$ will change its length and/or orientation in the presence of a velocity gradient.

Next, we consider the conservation of rest mass, which can be expressed as

$$\frac{D\rho}{Dt} = -\rho \vec{\nabla} \cdot \vec{\boldsymbol{u}}, \tag{B.4}$$

where ρ is the rest-mass density of the fluid. In ideal MHD the induction equation takes the well-known form

$$\frac{\partial \vec{\boldsymbol{B}}}{\partial t} = \vec{\nabla} \times \left(\vec{\boldsymbol{u}} \times \vec{\boldsymbol{B}}\right), \tag{B.5}$$

and the frozen-flux theorem states that the magnetic field lines are frozen in the fluid and can be identified with the worldlines of fluid elements. To see this, we use the following vector identity

$$\vec{\nabla} \times \left(\vec{\boldsymbol{u}} \times \vec{\boldsymbol{B}}\right) = \vec{\boldsymbol{B}} \cdot \vec{\nabla}\vec{\boldsymbol{u}} - \vec{\boldsymbol{B}}\left(\vec{\nabla} \cdot \vec{\boldsymbol{u}}\right) - \vec{\boldsymbol{u}} \cdot \vec{\nabla}\vec{\boldsymbol{B}} + \vec{\boldsymbol{u}}\left(\vec{\nabla} \cdot \vec{\boldsymbol{B}}\right), \tag{B.6}$$

together with $\vec{\nabla} \cdot \vec{\boldsymbol{B}} = 0$ in Eq. (B.5) to obtain

$$\frac{D\vec{\boldsymbol{B}}}{Dt} = \vec{\boldsymbol{B}} \cdot \vec{\nabla}\vec{\boldsymbol{u}} - \vec{\boldsymbol{B}}\left(\vec{\nabla} \cdot \vec{\boldsymbol{u}}\right). \tag{B.7}$$

Together with the conservation of mass, the above equation can then be written as

$$\frac{D}{Dt}\left(\frac{\vec{\boldsymbol{B}}}{\rho}\right) = \frac{\vec{\boldsymbol{B}}}{\rho} \cdot \vec{\nabla}\vec{\boldsymbol{u}}\,. \tag{B.8}$$

This is exactly the same equation satisfied by the separating vector $\vec{\boldsymbol{\xi}}$ [Eq. (B.3)]. Therefore a magnetic field line is advected and distorted by the fluid in the same way as a fluid element. If the fluid expansion takes place isentropically, the total entropy of the system remains constant and the entropy density s will satisfy the same conservation equation as the rest-mass density, i.e.,

$$\frac{Ds}{Dt} = -s\vec{\nabla} \cdot \vec{\boldsymbol{u}}\,. \tag{B.9}$$

From the arguments made above, it follows that the quantity $\vec{\boldsymbol{B}}/s$ will behave as the quantity $\vec{\boldsymbol{B}}/\rho$ and hence satisfy the equation

$$\frac{D}{Dt}\left(\frac{\vec{\boldsymbol{B}}}{s}\right) = \frac{\vec{\boldsymbol{B}}}{s} \cdot \vec{\nabla}\vec{\boldsymbol{u}}\,, \tag{B.10}$$

which is identical with Eq. (B.8) except ρ is replaced by s, i.e., for this case we also have the magnetic fluxes frozen in the system.

Appendix C. Limit for the log term

In this appendix we discuss how to evaluate the second term in Eq. (23) in the limit in which $a \to (1 + c_s^2)/2$, i.e., the limit

$$\lim_{a \to (1+c_s^2)/2} \frac{(\tau_0/\tau)^{1+c_s^2} - (\tau_0/\tau)^{2a}}{1 + c_s^2 - 2a}\,. \tag{C.1}$$

We first increase the power exponent a by an infinitesimal amount $\epsilon > 0$ and then take the limit $\epsilon \to 0$. In this case, Eq. (C.1) becomes

$$\lim_{\epsilon \to 0} \frac{(\tau_0/\tau)^{1+c_s^2} - (\tau_0/\tau)^{2(a+\epsilon)}}{1 + c_s^2 - 2\,(a+\epsilon)}\,, \tag{C.2}$$

and setting $a = (1 + c_s^2)/2$ we obtain the desired result

$$\left(\frac{\tau_0}{\tau}\right)^{1+c_s^2} \lim_{\epsilon \to 0} \frac{1 - (\tau_0/\tau)^{2\epsilon}}{(-2\epsilon)} = \left(\frac{\tau_0}{\tau}\right)^{1+c_s^2} \ln\left(\frac{\tau_0}{\tau}\right).$$

References

[1] A. Bzdak, V. Skokov, Phys. Lett. B 710 (2012) 171, arXiv:1111.1949 [hep-ph].
[2] W.T. Deng, X.G. Huang, Phys. Rev. C 85 (2012) 044907, arXiv:1201.5108 [nucl-th].
[3] D.E. Kharzeev, L.D. McLerran, H.J. Warringa, Nucl. Phys. A 803 (2008) 227, arXiv:0711.0950 [hep-ph].
[4] D.E. Kharzeev, H.U. Yee, Phys. Rev. D 83 (2011) 085007, arXiv:1012.6026 [hep-th].
[5] Y. Burnier, D.E. Kharzeev, J. Liao, H.U. Yee, Phys. Rev. Lett. 107 (2011) 052303, arXiv:1103.1307 [hep-ph].
[6] M.A. Stephanov, Y. Yin, Phys. Rev. Lett. 109 (2012) 162001, arXiv:1207.0747 [hep-th].
[7] D.T. Son, N. Yamamoto, Phys. Rev. D 87 (8) (2013) 085016, arXiv:1210.8158 [hep-th].
[8] J.W. Chen, S. Pu, Q. Wang, X.N. Wang, Phys. Rev. Lett. 110 (26) (2013) 262301, arXiv:1210.8312 [hep-th].
[9] A. Bzdak, V. Koch, J. Liao, Lect. Notes Phys. 871 (2013) 503, arXiv:1207.7327.
[10] D.E. Kharzeev, Prog. Part. Nucl. Phys. 75 (2014) 133, arXiv:1312.3348 [hep-ph].
[11] D.E. Kharzeev, arXiv:1501.01336 [hep-ph].
[12] X.G. Huang, J. Liao, Phys. Rev. Lett. 110 (23) (2013) 232302, arXiv:1303.7192 [nucl-th].
[13] S. Pu, S.Y. Wu, D.L. Yang, Phys. Rev. D 89 (8) (2014) 085024, arXiv:1401.6972 [hep-th].
[14] S. Pu, S.Y. Wu, D.L. Yang, Phys. Rev. D 91 (2) (2015) 025011, arXiv:1407.3168 [hep-th].
[15] P. Romatschke, U. Romatschke, Phys. Rev. Lett. 99 (2007) 172301; M. Luzum, P. Romatschke, Phys. Rev. C 78 (2008) 034915.
[16] H. Song, U.W. Heinz, Phys. Lett. B 658 (2008) 279; H. Song, U.W. Heinz, Phys. Rev. C 78 (2008) 024902.
[17] V. Roy, A.K. Chaudhuri, B. Mohanty, Phys. Rev. C 86 (2012) 014902, arXiv:1204.2347 [nucl-th].
[18] H. Niemi, G.S. Denicol, P. Huovinen, E. Molnar, D.H. Rischke, Phys. Rev. C 86 (2012) 014909, arXiv:1203.2452 [nucl-th].
[19] U. Heinz, C. Shen, H. Song, AIP Conf. Proc. 1441 (2012) 766, arXiv:1108.5323 [nucl-th].
[20] B. Schenke, S. Jeon, C. Gale, Phys. Rev. C 85 (2012) 024901, arXiv:1109.6289 [hep-ph].
[21] U. Gursoy, D. Kharzeev, K. Rajagopal, Phys. Rev. C 89 (5) (2014) 054905, arXiv:1401.3805 [hep-ph].
[22] B.G. Zakharov, Phys. Lett. B 737 (2014) 262, arXiv:1404.5047 [hep-ph].
[23] K. Tuchin, Phys. Rev. C 88 (2) (2013) 024911, arXiv:1305.5806 [hep-ph].
[24] S. Gupta, Phys. Lett. B 597 (2004) 57, arXiv:hep-lat/0301006.
[25] S.x. Qin, Phys. Lett. B 742 (2015) 358, arXiv:1307.4587.
[26] J.D. Bjorken, Phys. Rev. D 27 (1983) 140.

[27] R. Romero, J.M. Marti, J.A. Pons, J.M. Ibanez, J.A. Miralles, J. Fluid Mech. 544 (2005) 323, arXiv:astro-ph/0506527.
[28] M. Lyutikov, S. Hadden, Phys. Rev. E 85 (2012) 026401, arXiv:1112.0249 [astro-ph.HE].
[29] M. Gedalin, I. Oiberman, Phys. Rev. E 51 (1995) 5.
[30] X.G. Huang, A. Sedrakian, D.H. Rischke, Ann. Phys. 326 (2011) 3075, arXiv:1108.0602 [astro-ph.HE].
[31] B. Giacomazzo, L. Rezzolla, J. Fluid Mech. 562 (2006) 223, arXiv:gr-qc/0507102.
[32] B. Giacomazzo, L. Rezzolla, Class. Quantum Gravity 24 (2007) S235, arXiv:gr-qc/0701109.
[33] L. Rezzolla, O. Zanotti, Relativistic Hydrodynamics, Oxford University Press, Oxford UK, 2013.
[34] X.G. Huang, T. Kodama, T. Koide, D.H. Rischke, Phys. Rev. C 83 (2011) 024906, arXiv:1010.4359 [nucl-th].
[35] L.D. Landau, E.M. Lifshitz, Fluid Mechanics, Butterworth–Heinemann, Oxford, UK, 1987.